Magnetic and electrical transport anomalies of $RMAs_2$ (R = Pr and Sm, M = Ag and Au)

2009 J. Phys.: Condens. Matter 21 506004

(http://iopscience.iop.org/0953-8984/21/50/506004)

J. Phys.: Condens. Matter **21** (2009) 506004 (8pp) doi:10.1088/0953-8984/21/50/506004

Magnetic and electrical transport anomalies of $RMAs_2$ (R = Pr and Sm, M = Ag and Au)

K Mukherjee[1], E V Sampathkumaran[1], D Rutzinger[2], Th Doert[2] and M Ruck[2]

[1] Tata Institute of Fundamental Research, Homi Bhabha Road, Colaba, Mumbai 400005, India
[2] Department of Chemistry and Food Chemistry, Technische Universität Dresden, D-01062 Dresden, Germany

Received 30 September 2009, in final form 28 October 2009
Published 23 November 2009
Online at stacks.iop.org/JPhysCM/21/506004

Abstract

The results of magnetization, heat capacity and electrical resistivity (ρ) studies of the compounds $RMAs_2$ (R = Pr and Sm; M = Ag, Au), crystallizing in an $HfCuSi_2$-derived structure, are reported. $PrAgAs_2$ orders antiferromagnetically at $T_N = 5$ K. The Au analog, however, does not exhibit long range magnetic order down to 1.8 K. We infer that this is due to subtle differences in their crystallographic features, particularly noting that both the Sm compounds with identical crystal structures as that of the former order magnetically nearly at the same temperature (about 17 K). It appears that, in $PrAgAs_2$, $SmAgAs_2$ and $SmAuAs_2$, there is an additional magnetic transition at a lower temperature, as though the similarity in the crystal structure results in similarities in magnetism as well. The ρ for $PrAgAs_2$ and $PrAuAs_2$ exhibits a negative temperature coefficient in some temperature range in the paramagnetic state. $SmAuAs_2$ exhibits a magnetic Brillouin-zone gap effect in ρ at T_N, while $SmAgAs_2$ shows a well-defined broad minimum well above T_N around 45 K. Thus, these compounds reveal interesting magnetic and transport properties.

(Some figures in this article are in colour only in the electronic version)

1. Introduction

Following the discovery of superconductivity in the arsenide family in recent years, there have been explosive activities on arsenic-containing transition-metal compounds. In particular, the $ThCr_2Si_2$-derived tetragonal compounds have attracted a lot of interest in this respect. The arsenic compounds with 1:1:2 composition, e.g. the $HfCuSi_2$-type layered structure [1–3]—a defective variant of the $ThCr_2Si_2$ structure—however, has not been explored sufficiently for magnetic and superconducting anomalies, barring a few reports on Cu-based compounds $RCuAs_2$ (R = rare earth metals) [4–8]. Although corresponding Ag- and Au-based compounds were also identified [8–10], very little work has been reported on these compounds. Considering that the Cu-based compounds, even for those rare earths with 4f stability, have been reported to exhibit interesting properties, we considered it worthwhile to probe these Ag- and Au-containing compounds as well. We believe that the knowledge thus gathered would eventually contribute to a global understanding of the properties of the arsenide family. Among these Ag and Au compounds, interesting Kondo anomalies for Ce analogs have been reported in the recent literature [7]. Here we report the results of our investigation on the compounds $PrMAs_2$ and $SmMAs_2$ with M = Ag and Au. We find that the temperature (T) dependences of the electrical resistivity (ρ) of these compounds are interesting and not so commonly known for Pr and Sm compounds.

2. Crystallographic features

The crystal structures of these ternary compounds can be understood as variants of the tetragonal $HfCuSi_2$ type. In this structure, PbO-like layers of the coinage metals and arsenic are stacked along [001] with planar As sheets, separated by layers of the respective rare earth metals (figure 1). The undistorted $HfCuSi_2$ structure comprises As square layers. Due to a Peierls-like distortion, two different

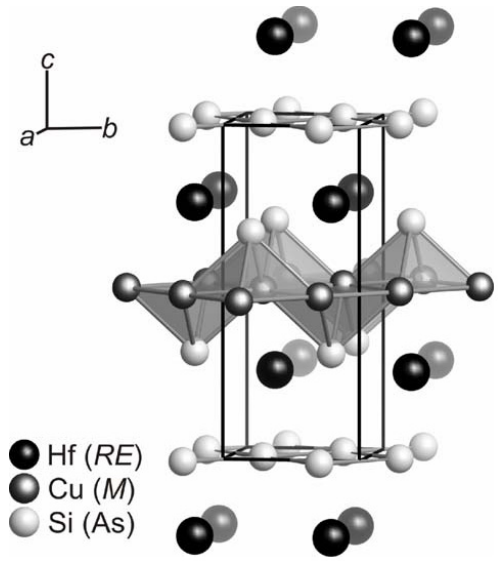

Figure 1. Crystal structure of $HfCuSi_2$.

structural variants are found for the title compounds: $PrAgAs_2$, $SmAgAs_2$ and $SmAuAs_2$ crystallize as twofold superstructures in orthorhombic space group *Pmcn* (no. 62) with the As atoms of their planar layers forming zigzag chains (figure 2), whereas $PrAuAs_2$ adopt a fourfold superstructure (orthorhombic space group *Pmca*) with *cis–trans* chains of As atoms (figure 2) [10].

3. Experimental details

The sample preparations were carried out in an argon-filled glove box (M. Braun, $p(O_2) \leqslant 1$ ppm, $p(H_2O) \leqslant 1$ ppm) with purification of argon by a molecular sieve and copper catalyst. Pieces of praseodymium (>99.9% purity, Treibacher AG) or samarium (99.9%, Chempur GmbH), freshly filed from rods of the respective rare earth metals, silver (powder, 99.9%, Chempur GmbH) or gold (powder, >99.9% purity, Chempur GmbH) and arsenic (powder, >99.997% metal-based, Aldrich; As_2O_3 removed by sublimation prior to use) were mixed in the atomic ratio of 1:1:2. The reactions were carried out in a sixfold excess of an LiCl/KCl flux (LiCl, KCl: powder, p. a., Merck, dried at 410 K in dynamic vacuum prior to use) in carbon crucibles which were sealed in evacuated silica ampules. The ampules were heated up to 1023 K for 48 h, annealed for 96 h and cooled to 623 K over a period of 192 h. The flux was removed with water and the polycrystalline products were washed with ethanol. The specimens thus obtained were shiny black platelets and stable in air. Pellets with 8 mm diameter and approximately 2 mm height were obtained at ambient temperature by pressing the polycrystals obtained by crushing under argon. The pellets were then sintered at 523 K for 24 h in evacuated sealed tubes.

X-ray powder diffraction patterns of the reaction products were recorded in order to check the sample purity. The measurements were performed in transmission geometry on a Stadi P diffractometer (Stoe & Cie., Darmstadt, Germany) equipped with an IP-PSD using Ge monochromatized Cu $K\alpha_1$ radiation. The evaluation of the patterns was done with the WinXPow program package [11]. All reflections can unambiguously be indexed (figure 3) with respect to theoretical patterns which were calculated on the basis of the structural models obtained from single-crystal data [10]. No lines of impurity phases were detected.

DC magnetization (M) measurements (1.8–300 K) were performed with the help of a commercial SQUID magnetometer (Quantum Design). The ρ measurements (1.8–300 K) in zero as well as in the presence of magnetic fields (H) were carried out employing a commercial physical properties measurements system (Quantum Design) and heat capacity (C) data were also collected with the same instrument by a relaxation method.

4. Results and discussion

We show the results for $PrAgAs_2$ in figures 4 and 5. The magnetic susceptibility (χ) obtained in a field of 5 kOe exhibits Curie–Weiss behavior in the range 30–300 K (figure 4(a)) and there is a deviation from this behavior at low temperatures (<30 K), which is usually attributed to crystal-field effects

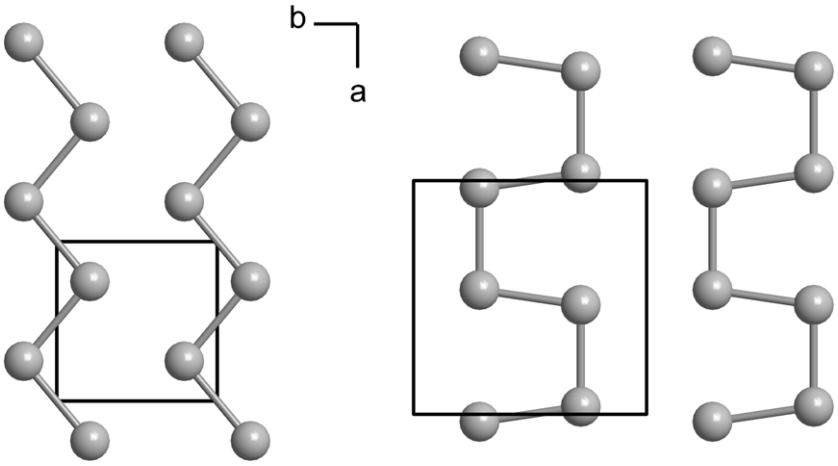

Figure 2. As layers of the compounds crystallizing as twofold superstructures of the $HfCuSi_2$ type in *Pmcn* (left) and as fourfold superstructures in *Pmca* (right).

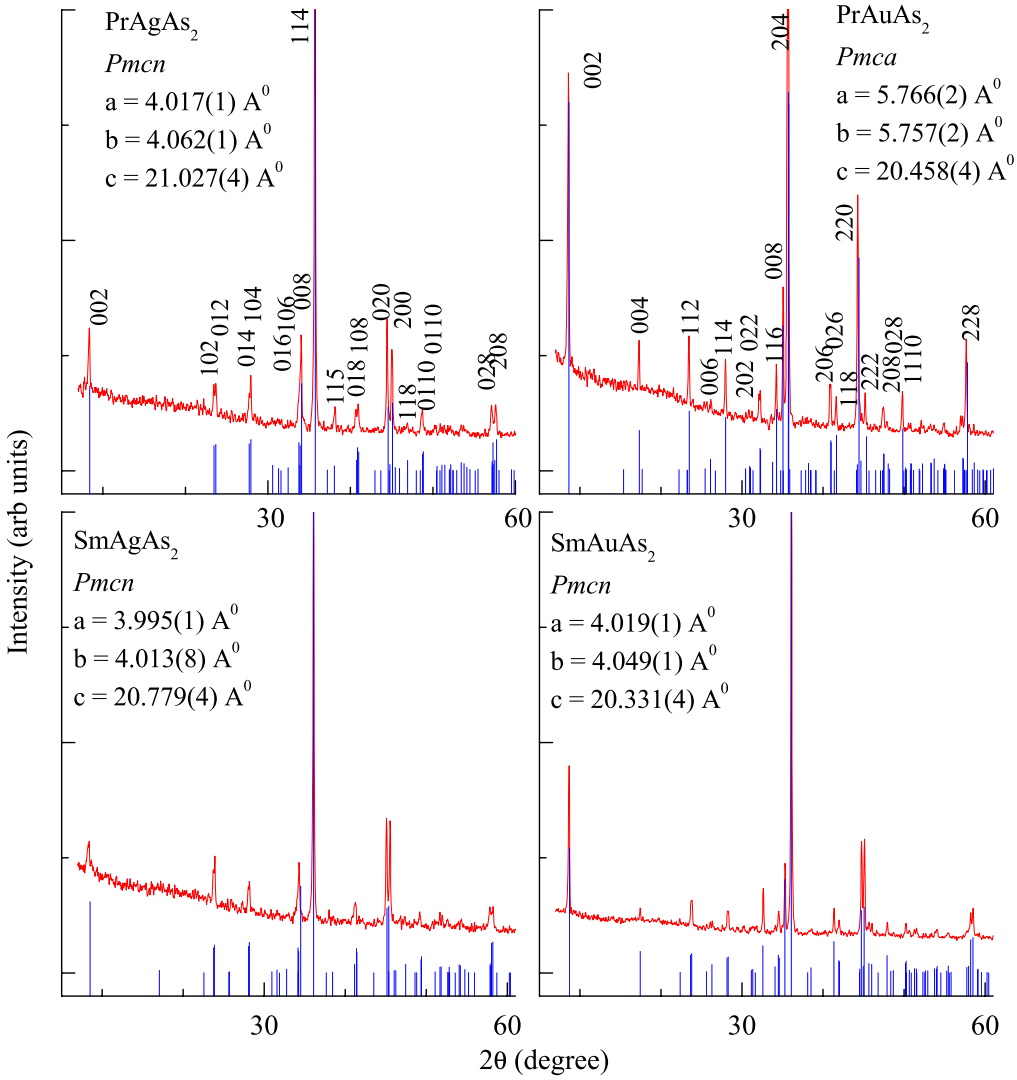

Figure 3. X-ray powder diffraction patterns of $RMAs_2$ (R = Pr and Sm, M = Ag and Au) obtained experimentally (curves) and by calculations (vertical bars) as mentioned in text. The lattice constants, a, b and c, are also included.

in the literature. The effective moment ($\mu_{\text{eff}} \sim 3.6\ \mu_B$) obtained from the linear region confirms the trivalency of Pr. The paramagnetic Curie temperature (θ_p) is found to be ~ -7 K and the negative sign indicates dominance of antiferromagnetic interactions. In order to understand the low temperature behavior, we show the plot of M/H as a function of T measured in a field of 100 Oe in figure 4(b). In this figure, there is a distinct peak at 5 K. Below 4 K, there is a bifurcation of the curves obtained under zero-field-cooled (ZFC) and field-cooled (FC) conditions (from 50 K) of the specimen. The $C(T)$ plot (figure 4(c)) reveals a prominent λ anomaly near 5 K, establishing long range magnetic order. Therefore, the bifurcation of ZFC–FC curves mentioned above is not due to spin-glass freezing. This conclusion was further confirmed by the absence of frequency dependence of ac susceptibility. Isothermal magnetization at 1.8 K exhibits a sharp increase for initial applications of the field (<5 kOe), followed by a sluggish variation at higher fields (figure 4(d)) and there is a weak irreversibility at low fields. This $M(H)$ behavior implies that there is a ferromagnetic component as well and therefore this compound could be classified as a canted antiferromagnet. However, it appears that there is a subtle change in the antiferromagnetic structure at 4 K, as shown by the differences in the $M(H)$ feature in the low-field range above and below 4 K. That is, at 1.8 K, there is a step in the virgin curve at low fields, whereas at 4.5 K this step is absent (see the inset of figure 4(d)). In addition, the $M(H)$ plot at 4.5 K is not hysteretic. A careful look at the derivative of ρ (see the inset of figure 5(a)) also offers support to the existence of two magnetic transitions in the close vicinity of 4 K, apart from the fact that the transport behavior is overall quite fascinating (figure 5(a)). ρ increases with decreasing temperature, exhibiting a maximum around 100 K and a minimum around 40 K followed by an upturn with a further decrease of temperature down to the lowest measured temperature. It appears that this is another example for the family of compounds exhibiting magnetic precursor effects [12]. The origin of the negative temperature coefficient of ρ in the paramagnetic state above 100 K is not clear and future studies should focus on whether this is

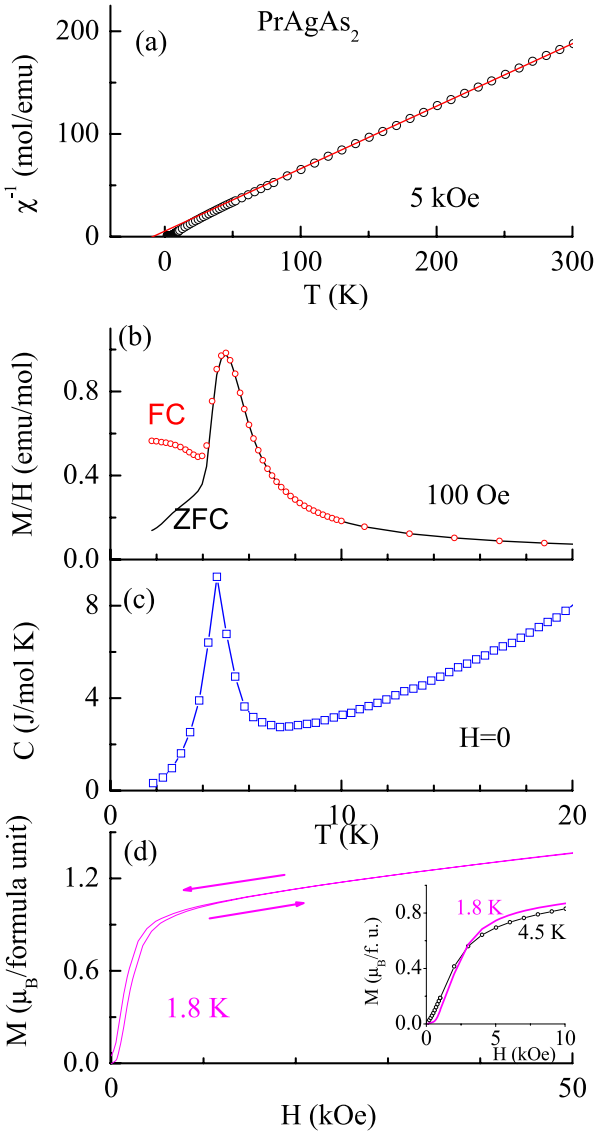

Figure 4. (a) Inverse magnetic susceptibility measured in a field of 5 kOe, (b) zero-field-cooled and field-cooled low-field magnetization, (c) heat capacity as a function of temperature and (d) isothermal magnetization as a function of magnetic field for 1.8 K is plotted for $PrAgAs_2$. In the inset of (d), the $M(H)$ behavior with increasing field at 1.8 and 4.5 K below 10 kOe are compared. In (a), a line is drawn through the Curie–Weiss region. Otherwise, the lines through the data points serve as guides to the eyes.

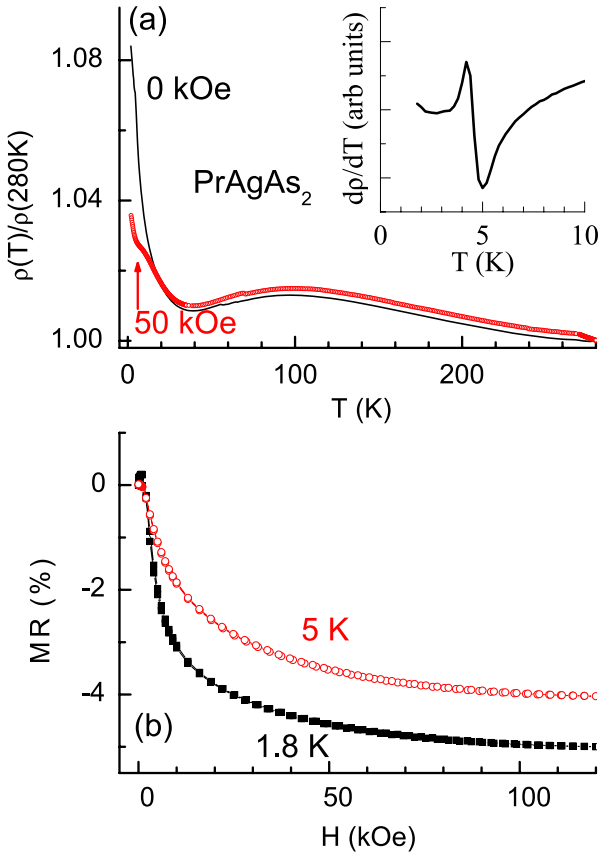

Figure 5. (a) Normalized electrical resistivity in zero and in 50 kOe as a function of temperature for $PrAgAs_2$. (b) For the same sample, the magnetoresistance as a function of magnetic field at 1.8 and 5 K is plotted. The lines through the data points serve as guides to the eyes. In the inset of (a), the temperature derivative of electrical resistivity is plotted to highlight the changes in slopes at 4 and 5 K.

due to Pr 4f hybridization effects. We have also extended low-field (100 Oe) magnetization studies up to 250 kOe to explore whether there is any other magnetic anomaly around 100 K, but we could not detect any. With respect to the behavior near T_N, it should be noted that there is no fall of ρ below T_N and the upturn keeps continuing down to the lowest measured temperature. This establishes that, at T_N, there is a magnetic pseudogap formation. This is further established by the observation that an application of magnetic field gradually decreases ρ (figure 5(b)) resulting in negative magnetoresistance (MR $= [\rho(H) - \rho(0)/\rho(0)]$), which is prominent below T_N only (compare in-field and zero-field curves, figure 5(a)). Despite the fact that there is no fall due to loss of the spin-disorder contribution at the onset of the magnetic transition, the inset of figure 5 reveals that there are distinct changes in the slopes of $\rho(T)$ at 4 and 5 K, thereby revealing that the ZFC–FC bifurcation of $\chi(T)$ curves at 4 K in figure 4(b) must have its origin in a subtle change in the magnetic structure (supporting the inference from the $M(H)$ curve in the low-field range, made above). These results overall establish that this compound is an antiferromagnet with interesting transport anomalies, even in the paramagnetic state.

With respect to $PrAuAs_2$, χ monotonically increases with decreasing T, exhibiting Curie–Weiss behavior down to 20 K (figure 6(a)) typical of trivalent Pr ions. The sign and the magnitude of θ_p is the same as in $PrAgAs_2$. There is no difference in low-field ZFC and FC curves down to 1.8 K (figure 6(b)) and χ continues to rise down to 2 K. These features indicate that there is no long range magnetic order down to 1.8 K. This is consistent with the absence of any λ anomaly in $C(T)$ (figure 6(c)). However, a plot of C/T reveals a gradual fall below 7 K. In addition, isothermal M at 1.8 K shows a marginal deviation at high fields from the low-field linear behavior (see the inset in figure 6(a)). In order to understand these features, we have taken MR data as a function of H (figure 7(a)). It is found that MR (with negative sign) varies quadratically with H initially typical of paramagnets above 10 K, as shown for 20 K in figure 7(a). However,

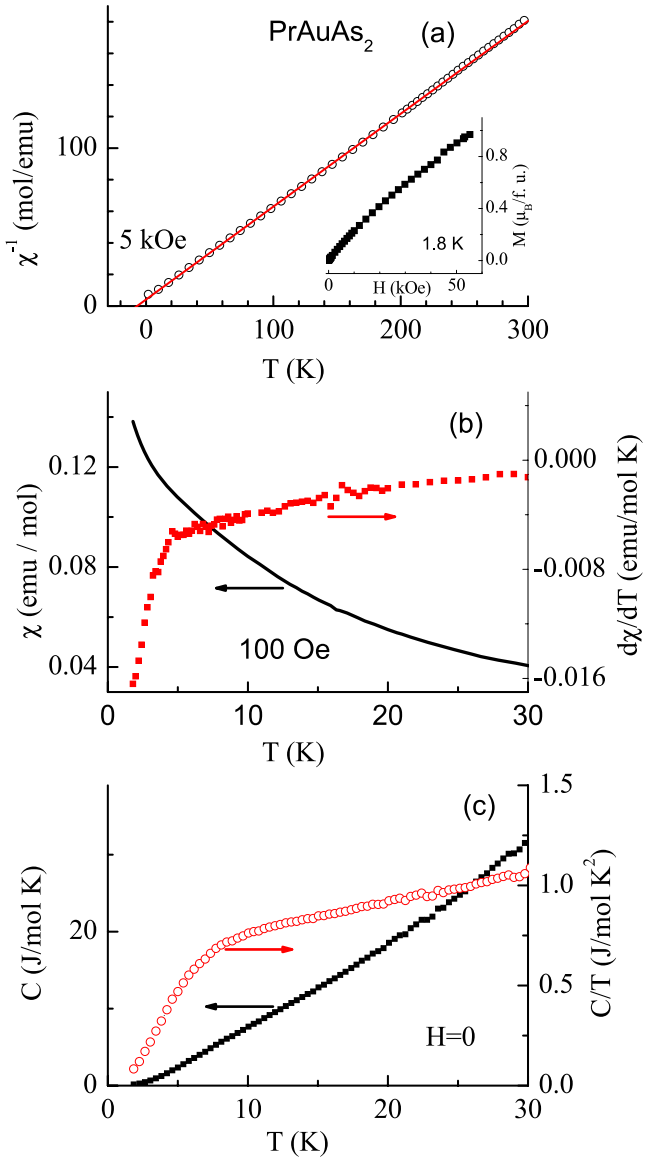

Figure 6. (a) Inverse magnetic susceptibility (χ) measured in a field of 5 kOe, (b) χ and $\mathrm{d}\chi/\mathrm{d}T$ as a function of temperature measured in a field of 100 Oe and (c) heat capacity data as a function of temperature for $PrAuAs_2$. In the inset of (a), isothermal magnetization at 1.8 K is plotted. A continuous line through the Curie–Weiss region is drawn in (a).

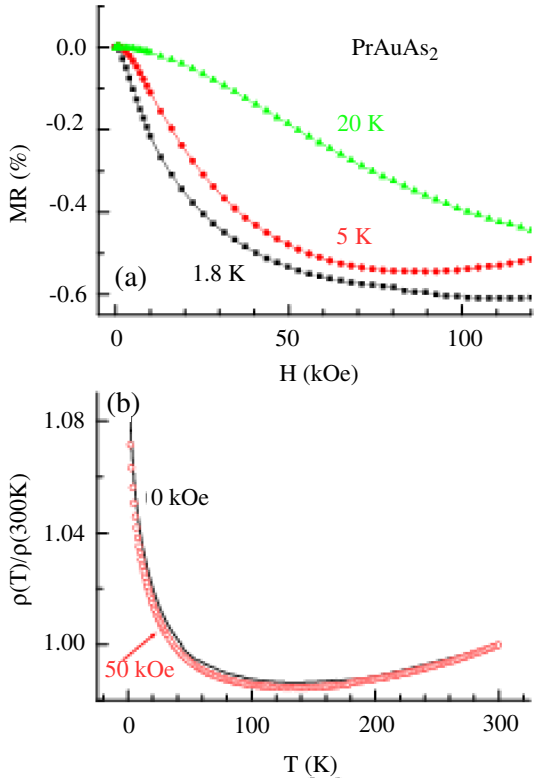

Figure 7. (a) Magnetoresistance as a function of magnetoresistance at 1.8, 5 and 20 K, and (b) normalized electrical resistivity as a function of temperature in zero and in 50 kOe for $PrAuAs_2$. Continuous lines through the data points are drawn as guides to the eyes.

as the temperature is lowered below 7 K, the variation of MR is steeper (with the negative sign of MR), as though there is a magnetic ordering. Spin-glass behavior is ruled out considering the absence of a bifurcation of ZFC and FC χ curves. A way to reconcile this behavior is to propose that there are short range correlations developing gradually below 7 K in this compound. In fact, the temperature derivative of χ shows a significant change as shown in figure 6(b) around this temperature which appears to endorse this inference. In figure 7(b), we show the $\rho(T)$ behavior in zero field and in 50 kOe. While the slope of ρ is positive above about 150 K, there is a broad, but distinct, minimum around 100 K with the upturn persisting down to 2 K. These features persist even for $H = 50$ kOe. If one assumes that long range magnetic ordering sets in below 1.8 K, then the low temperature increase could be of the same origin as in the Ag analog. Experiments at low temperatures (<1.8 K) are warranted for this compound to understand it better. We believe that the suppression of long range magnetic ordering in $PrAuAs_2$ with respect to the Ag analog, despite similar values of θ_p, is in some way related to the fourfold superstructure with *cis–trans* chains of As atoms (possibly inducing magnetic frustration in some fashion). This inference gains further support from the similarities in the magnetism of Sm compounds.

The results on $SmAgAs_2$ are shown in figures 8 and 9. It is a well-known fact that Sm in its trivalent state exhibits complex temperature-dependent behavior due to narrow multiplet widths and crystal-field splitting, as a result of which Curie–Weiss behavior in the paramagnetic state is unexpected. Our aim here is to focus on the low temperature behavior in the vicinity of the magnetic transition. It is obvious from figure 8(a) that there is a peak in $\chi(T)$ at ∼16 K due to the onset of magnetic ordering and another upturn below 8 K. This is observed irrespective of whether the specimen was cooled in zero field or in a field. While there is a prominent λ anomaly in C near 16 K (figure 8(b)) establishing long range magnetic ordering at this temperature, the feature near 8 K (marked by an arrow) is, however, weak. Possibly the entropy associated with the 8 K transition is negligible. It is, however, important to ensure that this transition is not due to an impurity. The $\rho(T)$ behavior in this regard is quite helpful in resolving this.

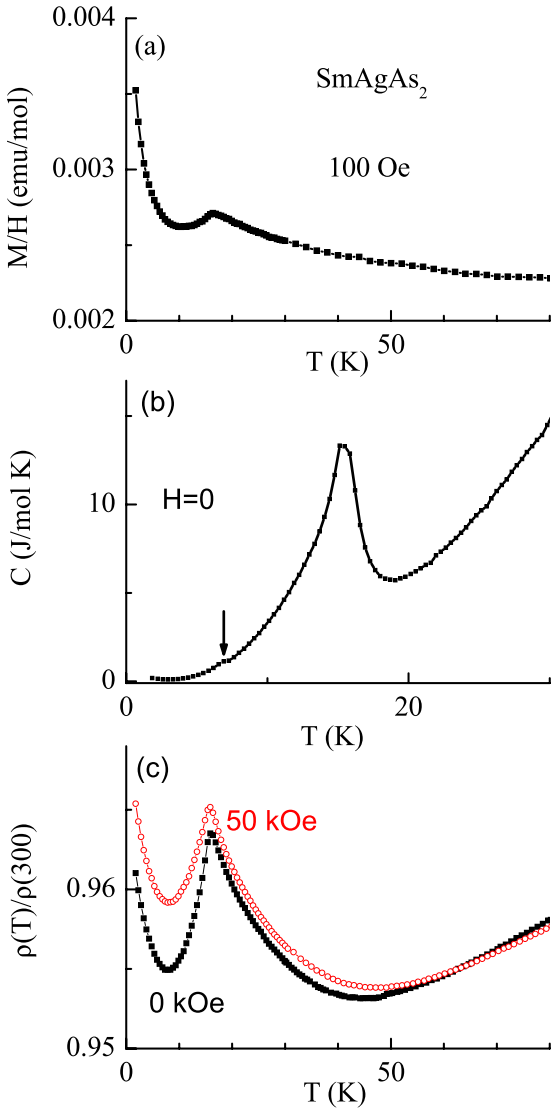

Figure 8. Temperature dependence of (a) magnetization, (b) heat capacity and (c) normalized electrical resistivity (in zero field and in 50 kOe) in the vicinity of the magnetic transition for $SmAgAs_2$. The lines through the data points serve as guides to the eyes.

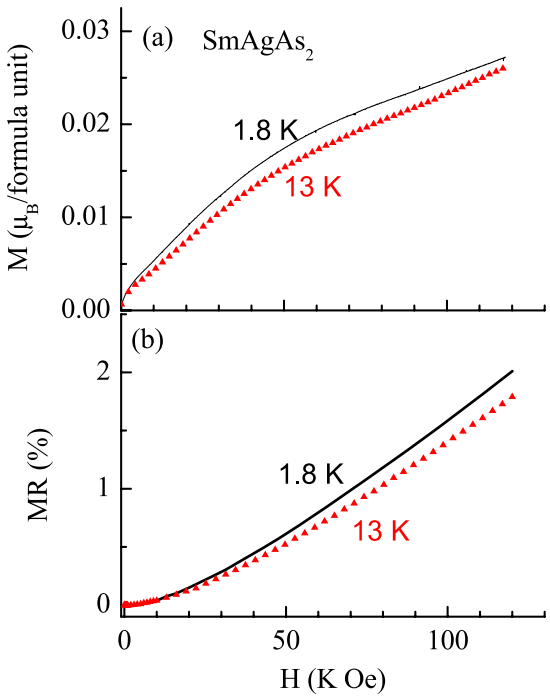

Figure 9. (a) Isothermal magnetization and (b) magnetoresistance as a function of magnetic field at 1.8 and 13 K for $SmAgAs_2$.

In figure 8(c), in addition to a fall below 16 K due to a loss of spin-disorder contribution, there is an upturn below 8 K. This 8 K upturn in ρ cannot be due to any impurity; if the 8 K feature in χ and C is attributed to impurity, the positive temperature coefficient of the main magnetic phase should have resulted in a continuous fall of ρ below 8 K as well. A semiconducting impurity phase cannot dominate transport behavior when its fraction is small (if inferred from the strength of the C feature). Therefore, we tend to believe that there is another magnetic feature coming from the $SmAgAs_2$ phase only and the 8 K upturn may arise from a magnetism-induced pseudogap setting in at this temperature due to possible spin reorientation. The change in spin alignment must be a subtle one, as there is no dramatic difference in the nature of the $M(H)$ curves above and below 8 K (compare the curves in figure 9(a) for these temperatures). M increases in a sluggish manner with H without any hysteresis. From this, we infer that the magnetic ordering is of an antiferromagnetic type in this compound. We also wanted to see whether MR can throw some light on this conclusion, but MR appears to be dominated by a conduction electron contribution, as indicated by its quadratic field dependence with a positive sign. The most interesting observation for this compound is that $\rho(T)$ exhibits a minimum around 50 K, which is three times that of T_N (~16 K), which could not be suppressed by an application of a magnetic field of 50 kOe (figure 8(c)).

In the case of $SmAuAs_2$, the features attributable to two magnetic transitions are visible in $\chi(T)$ (see figure 10) in the form of flattening around (T_N =)17 K, followed by an upturn below about 12 K. There is no difference between ZFC and FC curves. The fact that these are bulk magnetic transitions is confirmed by prominent peaks in $C(T)$ at these temperatures (figure 10(b)). There is an upturn in $\rho(T)$ below 17 K (figure 10(c)) due to magnetic Brillouin-zone formation, thereby indicating that the magnetic transition at this temperature is of an antiferromagnetic type. However, this gap effect appears to diminish as soon as the second transition sets in, as indicated by a gradual fall of ρ around this temperature. Interestingly, further lowering of temperature below 6 K results in a negative temperature coefficient of ρ. These features are not altered in a field of 50 kOe. Thus, it appears that there are interesting changes in the Fermi surface with varying temperature below T_N. It is to be noted that, below T_N, $M(H)$ curves are non-hysteretic varying gradually with H without any tendency for saturation (figure 11(a)) similar to that for $SmAgAs_2$. We would like to add that the sign of MR is positive in the entire temperature range below T_N (see figure 11(b)) varying nearly quadratically with H similar to $SmAgAs_2$. With respect to the transport behavior in the

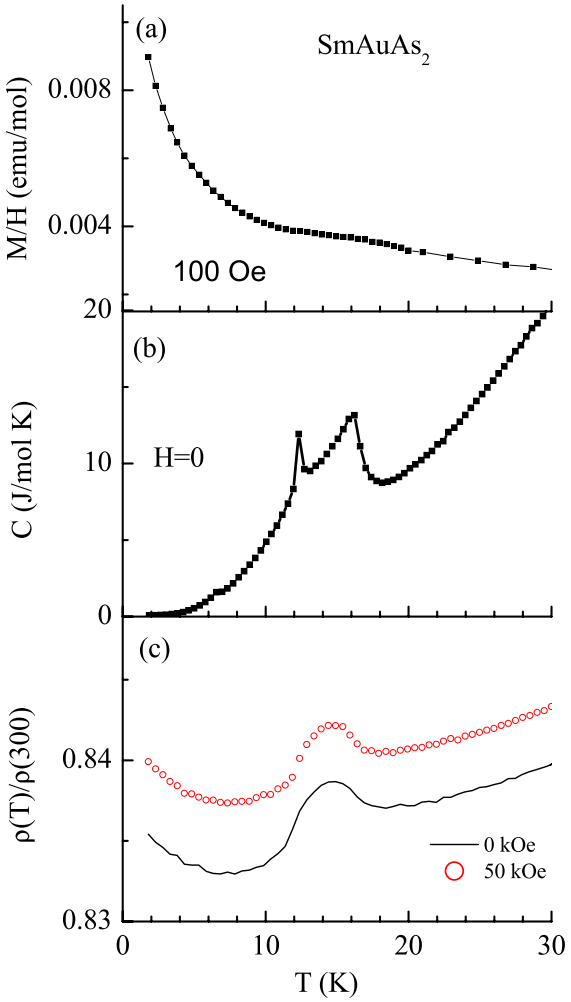

Figure 10. (a) Low-field magnetic susceptibility, (b) heat capacity and (c) normalized electrical resistivity as a function of temperature for $SmAuAs_2$.

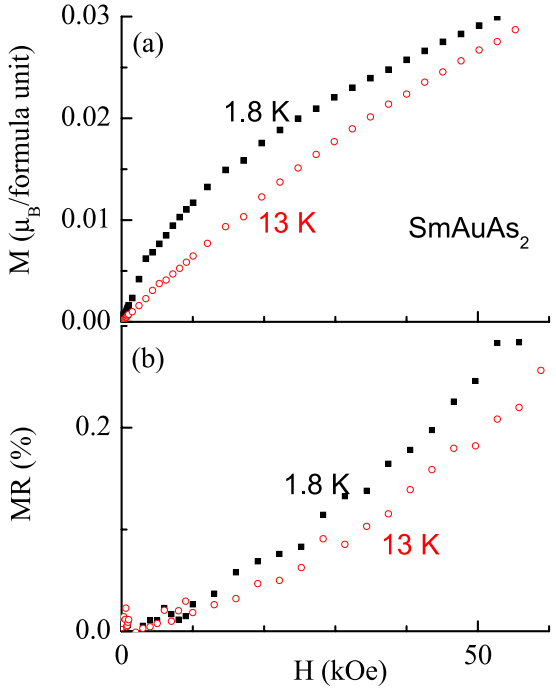

Figure 11. (a) Isothermal magnetization and (b) magnetoresistance at 1.8 and 13 K for $SmAuAs_2$.

paramagnetic state, unlike in $SmAgAs_2$, ρ is metallic-like without any minimum.

5. Summary

The magnetic and transport properties of ternary arsenides, $RMAs_2$ (R = Pr and Sm, M = Ag and Au) have been investigated. All, except $PrAuAs_2$, order antiferromagnetically at low temperatures with complex electrical resistivity behavior. It is intriguing to note that $PrAgAs_2$ and the Sm compounds are characterized by similar magnetic anomalies in the sense that there are two magnetic transitions, as though similarity in crystal structure determines this magnetic behavior. Since the onset of magnetic transition occurs at nearly the same temperature for both the Sm compounds with the same crystallographic features, a suppression of magnetic ordering in the $PrAuAs_2$ in comparison with $PrAgAs_2$ (despite the same value of θ_p) may be attributable to subtle structural differences, possibly in the superstructure features, as outlined in section 2, between these two Pr compounds. A point being stressed is that, even in the paramagnetic state, the transport behavior is interesting in the sense that a negative temperature coefficient of $\rho(T)$ far above T_N is observed in all cases except $SmAuAs_2$, with insensitivity to application of a magnetic field. Similar behavior was reported for $RCuAs_2$ (Sampathkumaran *et al* [12]). Such a feature prior to an onset of long range magnetic order is of theoretical interest [13, 14] and it is possible to explain its presence in some ferromagnetic systems [13]. Free-electron scattering on collective excitations from crystal-field levels [14] was proposed as an explanation in all magnetic materials. It is, however, not clear whether insensitivity of the $\rho(T)$ minimum to applications of magnetic fields can be explainable within this theory. In addition, among the two Sm systems in the same family, only one member exhibits this anomaly. It therefore appears that more theoretical work is required to address this transport anomaly.

Acknowledgments

We thank Sitikantha D Das and Kartik K Iyer for their help while carrying out experiments.

References

[1] Brylak M, Möller M H and Jeitschko W 1995 *J. Solid State Chem.* **115** 305
[2] Jemetio J-P, Doert Th, Rademacher O and Böttcher P 2002 *J. Alloys Compounds* **338** 93
[3] Mozharivskyj Y, Kaczowrowski D and Franzen H 2000 *J. Solid State Chem.* **155** 259
[4] Sampathkumaran E V, Sengupta K, Rayaprol S, Iyer Kartik K, Doert Th and Jemetio J P F 2003 *Phys. Rev. Lett.* **91** 036603
[5] Sengupta K, Sampathkumaran E V, Nakano T, Hedo M, Abliz M, Fujiwara N, Uwatoko Y, Rayaprol S, Shigetoh K, Takabatake T, Doert Th and Jemetio J P F 2004 *Phys. Rev.* B **70** 064406

[6] Sampathkumaran E V, Ekino T, Ribeiro R A, Sengupta K, Nakano T, Hedo M, Fujiwara N, Abliz M, Uwatoko Y, Rayaprol S, Doert Th and Jemetio J P F 2005 *Physica* B **359–361** 108
[7] Slazska M and Kaczorowski D 2008 *J. Alloys Compounds* **451** 464
[8] Demchyna R, Jemetio J P F, Prots Yu, Doert Th, Akselrud L G, Schnelle W, Kuzma Yu and Grin Yu 2004 *Z. Anorg. Allg. Chem.* **630** 635
[9] Eschen M and Jeitshsko W 2003 *Z. Naturforsch.* b **58** 399
[10] Rutzinger D, Bartsch C, Dörr M, Rosner H, Neu V, Doert Th and Ruck M *J. Solid State Chem.* at press
[11] 1999 *WinXPow, Program for the Collection and the Evaluation of X-ray Powder Data* Stoe & Cie. GmbH, Darmstadt
[12] See, for instance, Mallik R, Sampathkumaran E V, Strecker M and Wortmann G 1998 *Europhys. Lett.* **41** 315
Saha S R, Sugawara H, Matsuda T D, Sato H, Mallik R and Sampathkumaran E V 1999 *Phys. Rev.* B **60** 12162
Sampathkumaran E V, Sengupta K, Rayaprol S, Iyer Kartik K, Doert Th and Jemetio J P F 2003 *Phys. Rev. Lett.* **91** 036603
Sengupta K, Rayaprol S and Sampathkumaran E V 2005 *Europhys. Lett.* **69** 454
[13] Eremin I, Thalmier P, Fulde P, Kremer R K, Ahn K and Simon A 2001 *Phys. Rev.* B **64** 064425
[14] Szukiel A E and Peisert J 2009 *Physica* B **404** 1465